BISTATIC RADAR OBSERVATIONS OF THE MOON USING THE ARECIBO OBSERVATORY & MINI-RF ON LRO. D. B. J. Bussey[1], G. W. Patterson[1], R. Schulze[1], D. E. Wahl[2], M. Nolan[3], J. R. Jensen[1], F. S. Turner[1], D. A. Yocky[2], C. V. Jakowatz[2], I. Erteza[2], L. Carter[4], C.D. Neish[4] and the Mini-RF Team, [1]Applied Physics Laboratory, Laurel MD 20723, [2]Sandia National Laboratory, Albuquerque NM, [3]Arecibo Observatory, Arecibo PR, [4]NASA Goddard Space Flight Center, Greenbelt, MD.

Introduction: The Mini-RF team is acquiring bistatic radar measurements of the lunar surface to understand the scattering properties of materials as a function of bistatic angle. These observations have produced the first lunar radar images ever collected with non-zero bistatic angles. The goal of these observations is to test the hypothesis that some permanently shadowed areas near the lunar poles contain water ice.

Rationale: The bistatic angle is determined by the positions and orientations of the radar transmitter and receiver. For radar observations that use the same antenna to transmit and receive a signal, the bistatic angle is zero, and they are referred to as monostatic. NASA's Mini-RF instrument on the Lunar Reconnaissance Orbiter is currently operating in a bistatic mode with the Arecibo Observatory acting as the transmitter and the Mini-RF antenna acting as the receiver. In this mode, Arecibo transmits a circular polarized S-band signal at a transmitted power of 200 kW. The portion of the signal reflected off the lunar surface and into the Mini-RF antenna is received in orthogonal linear polarizations as well as their relative phase. This architecture is equivalent to the hybrid dual-polarimetric architecture of the monostatic mode for the Mini-RF instrument [1] and, therefore, allows for the calculation of the Stokes parameters (S_1, S_2, S_3, S_4) that characterize the backscattered signal (and the products derived from those parameters).

The circular polarization ratio,

$$CPR = (S_1 - S_4)/(S_1 + S_4)$$

is a product of the Stokes parameters that is often utilized in analyses of planetary radar data [2-5]. This ratio provides an indication of surface roughness, as determined by the distribution of surface and buried wavelength-scale scatterers (*e.g.*, boulders). Typical dry lunar surface has a CPR value less than unity [3]. Higher CPR signals can result from multiple-bounce backscatter off rocky surfaces or from the combined volume scattering and coherent backscatter opposition effects (CBOE) of an ice/regolith mixture [3]. High CPR caused by a rocky surface should be relatively insensitive to the bistatic angle, whilst high CPR caused by ice should be very sensitive to the bistatic angle. I.e., CPR values should decrease abruptly for ice/regolith mixtures at bistatic angles greater than about 1-2° (figure 1).

Monostatic radar data of the lunar surface clearly show that craters and their ejecta typically have elevated CPR values, with respect to background lunar terrain [6]. This is especially characteristic of young, fresh craters and indicates that the crater and its ejecta have a higher fraction of cm- to m-scale scatterers at the surface and/or buried to depths that scale with the wavelength of the transmitted radar signal.

Recent work using Mini-RF on LRO and Mini-SAR data from India's lunar Chandrayaan-1 spacecraft [7] (2008-9), has shown that some permanently shadowed 'anomolous' craters near both poles show elevated CPR interior to the crater rim but low CPR exterior to the crater rim [3,4]. This has been interpreted as consistent with RF backscatter caused by crater interior deposits of an ice/regolith mixture. However, as CPR is a non-unique descriptor of physical composition, we cannot be certain with existing data alone that the anomalous scattering is caused by the presence of ice.

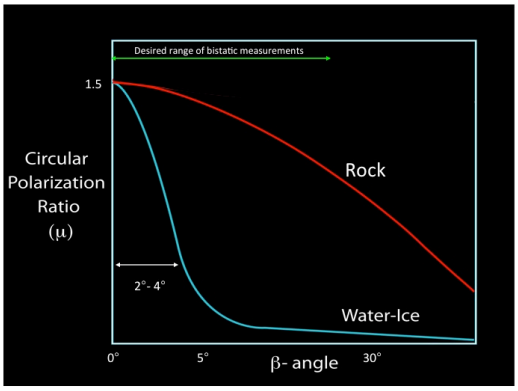

Figure 1. Predicted behavior of CPR versus beta angle for both rocky terrains and an ice/regolith mixture.

Observations: To further investigate the nature of the RF signature associated with anomalous craters, we are imaging non-polar and polar targets that have high monostatic CPR values for a range of bistatic angles (figure 2, 3). Non-polar targets are used to characterize how CPR varies as a function of bistatic angle for craters deposits in which the presence of water ice is not expected (red line in figure 1)

Non-polar craters for which data has been acquired, to date, include the 4 km diameter crater La Condamine S (57.3°N, 25.2°W) and the 31 km diameter crater Kepler (8.1°N, 38.0°W - figure 3), The bistatic angle coverage of these targets ranges from 0° to 12°. Initial results have been surprising in that CPR values of the rough ejecta blankets of these craters have been lower than expected, indicating that CPR

may vary with bistatic angle more than predicted.

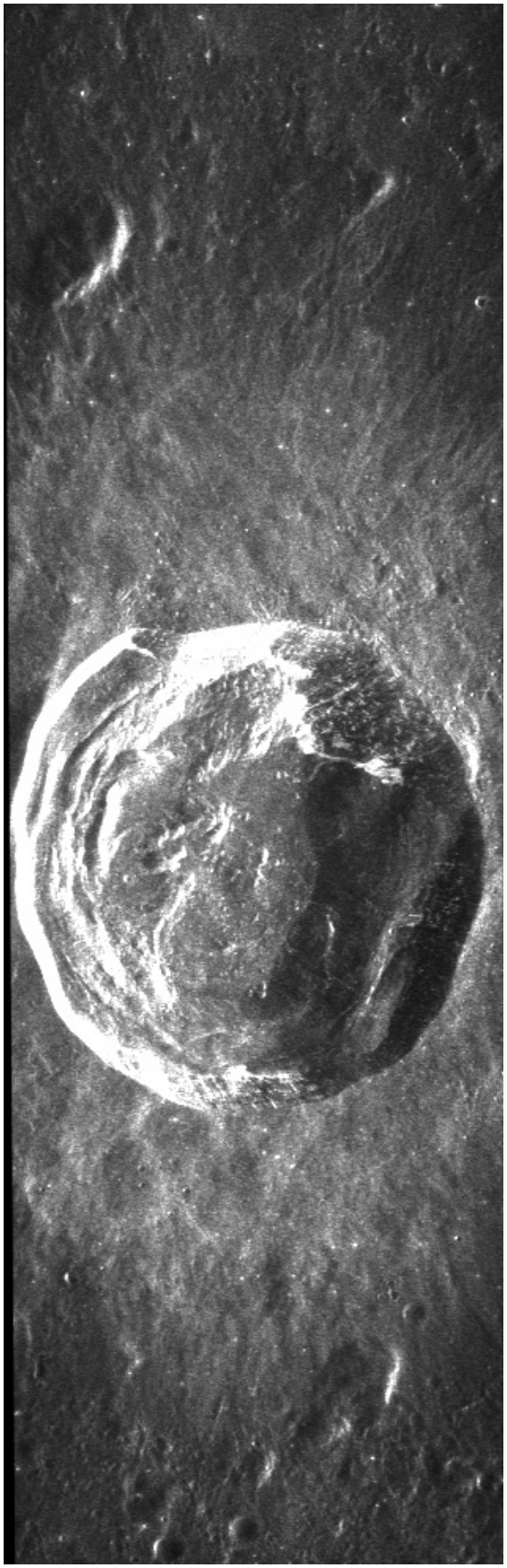

Figure 2. Bistatic radar image of the 31 km diameter crater Kepler.

However, the effects of variations in incidence and emission angle across these targets and how that relates to changes in bistatic angle still need to analyzed. The key goal of these non-polar observation is to characterize the scattering properties of a rough surface as a function of bistatic angle so that we can analyze high-CPR permanently shadowed regions to determine if their radar signature behaves differently.

We are looking to see if monostatic high-CPR polar craters have high or low values in the bistatic data. If we find areas that become low only in the bistatic data then this provides strong supporting evidence that these are ice deposits.

Conclusions: Using Arecibo and Mini-RF we have acquired the first ever planetary bistatic radar images of the lunar surface. These data provide a unique new piece of evidence to determine if the Moon's polar craters contain ice.

Figure 3. Bistatic image of a portion of the south polar region. Shackleton crater is visible in the top right.

References: [1] Raney, R. K. et al. (2011), *Proc. of the IEEE*, 99, 808-823; [2] Campbell B. et al., Nature, 2006; [3] Spudis P.D. et al., GRL 2010; [4] Spudis et al. (2013), *Icarus*, submitted; [5] Carter et al. (2012), JGR, 117, E00H09; [6] Ghent et al. (2010), *Icarus*, 209, 818-835; [7] Goswami and Annadurai (2009), Current Science 96, 486;